Biogeosciences, 22, 5247–5256, 2025
https://doi.org/10.5194/bg-22-5247-2025

Biogeosciences Open Access EGU

BG Letters

Extensive fire-driven degradation in 2024 marks worst Amazon forest disturbance in over 2 decades

Clément Bourgoin[1], René Beuchle[1], Alfredo Branco[1], João Carreiras[2], Guido Ceccherini[3], Duarte Oom[1], Jesus San-Miguel-Ayanz[1], and Fernando Sedano[1]

[1]European Commission, Joint Research Centre (JRC), Ispra, 21027, Italy
[2]VASS Italy, Torino, 10100, Italy
[3]Engineering Ingegneria Informatica S.p.A., Roma, 00144, Italy

Correspondence: Clément Bourgoin (clement.bourgoin@ec.europa.eu)

Received: 16 April 2025 – Discussion started: 5 May 2025
Accepted: 9 July 2025 – Published: 8 October 2025

Abstract. The Amazon rainforest, historically fire-resistant, is experiencing an alarming increase in wildfires due to climate extremes and human activity. The 2023–2024 drought, surpassing previous records, combined with forest fragmentation, has dramatically heightened fire vulnerability. Analysing the Tropical Moist Forest (TMF) and Global Wildfire Information System (GWIS) datasets, we found a 152 % surge in forest disturbances from deforestation and degradation in 2024, reaching a 2-decade peak of 6.64 Mha (million hectares). Forest degradation, particularly large-scale degradation linked to fires, increased by over 400 %, largely exceeding deforestation. Brazil and Bolivia experienced the most severe impacts, with Bolivia seeing 9 % of its intact forest burned in 2024. Fire-driven forest degradation in the Pan-Amazon released 791 ± 86 Mt CO_2 (million tonnes of carbon dioxide equivalent, ± 1 standard deviation) in 2024, a 7-fold increase compared to the previous 2 years, surpassing emissions from deforestation. The escalating fire occurrence, driven by climate change and unsustainable land use, threatens to push the Amazon towards a catastrophic tipping point. Urgent, coordinated efforts are crucial to mitigate these drivers and to prevent irreversible ecosystem damage.

1 Introduction

The Amazon's humid forests, once resistant to fire due to their high humidity and regular rainfalls, are undergoing an alarming and rapid transformation. The unprecedented 2023–2024 drought, which shattered the 2010 and 2015–2016 records with its dramatic precipitation deficit and prolonged, intense heatwaves (Kornhuber et al., 2024, Marengo et al., 2024), has severely stressed the region's delicate ecological balance. This has resulted in diminished surface water resources, reduced soil moisture, and stressed vegetation, creating conditions that significantly elevate the likelihood and severity of forest fires (Barlow et al., 2020). This already precarious situation is further compounded by the forest's degraded state, a consequence of extensive deforestation and habitat fragmentation, selective logging, and past fire events, leaving it increasingly susceptible to future, potentially catastrophic wildfires (Bourgoin et al., 2024). This degraded state also sets in motion a series of detrimental feedback loops: the increased tree mortality due to edge effects acts as readily available fuel for fires, while fragmentation facilitates greater access for hunting and resource extraction, both of which contribute directly to tree mortality and heightened fire incidence (Matricardi et al., 2012; Condé et al., 2019).

Natural fires, such as those caused by lightning, are extremely rare in the Amazon. Most fire ignitions in the Amazon result from human activity. Among them, "escape fires" are fires that accidentally spread into neighbouring forests from recently cleared deforested land or burned pastures, causing forest degradation (Cano-Crespo et al., 2015), or that are deliberately set to pave the way for potential future illegal deforestation (Andela et al., 2022). The consequences of forest fires are multifaceted, directly harming plant and animal life, affecting the integrity of once-intact forests, and causing further damage to already degraded areas (Lapola et al., 2023). Recent degradation from fire shows a 60 % decrease

in aboveground biomass density compared to adjacent intact forests, releasing substantial greenhouse gases and accelerating global warming (Bourgoin et al., 2024). Forest fires also have severe implications for indigenous peoples, who face the threat of losing intact forest within their territories and experience severe respiratory health impacts from smoke exposure, often more so than other residents of the Amazon (Rorato et al., 2022).

As Amazon fire threats grow, rapid and accurate detection is paramount. Distinguishing forest degradation fires from agricultural fires is key in assessing impacts on people, ecosystems, and climate and in developing effective mitigation measures. To address this need, we analysed the Tropical Moist Forest (TMF) dataset, updated through 2024 (Vancutsem et al., 2021). This dataset, leveraging the Landsat archive from 1990 onwards, identifies forest disturbances, classifying them as either deforestation or degradation (Vancutsem et al., 2021; see the Appendix for more details). It further classifies degradation into small-scale (a proxy for windthrow and selective logging) and large-scale events (a proxy for forest fire and drought). To enhance our understanding of fire-driven degradation, we integrated the Global Wildfire Information System (GWIS) burnt-area data, which rely on Moderate-Resolution Imaging Spectroradiometer (MODIS) and Visible Infrared Imaging Radiometer Suite (VIIRS) thermal anomalies from 2012 to 2024 (San-Miguel et al., 2023). We estimated carbon dioxide (CO_2) emissions from fire-driven degradation and deforestation, along with their associated uncertainties, following the IPCC (2006) guidelines and incorporating the ESA CCI 2021 Above Ground Biomass dataset (Santoro and Cartus, 2024).

2 Results

Our results show that the area of the Pan-Amazon region affected by forest disturbances dramatically increased by 152 % from 2023 to 2024, reaching a 2-decade peak of 6.64 Mha (million hectares) (Fig. 1a). Despite a 20 % decrease in deforestation in 2024 compared to the 2019–2023 average, forest degradation surged by over 400 %, generally becoming increasingly prominent and surpassing deforestation by 1.3, 1.7, and 4.2 times in the 2010, 2016, and 2024 extreme climatic events. Large-scale degradation totalled 3.31 Mha in 2024, representing a 1077 % increase compared to the annual average for the 2019–2023 period. This coincided with a 1461 % increase in burned forest area, totalling 3.56 Mha, 80 % of which overlaps with TMF large-scale degradation (more details on the integration of TMF-GWIS datasets can be found in Appendix A3).

Brazil suffered the largest absolute large-scale degradation in 2024 (1.66 Mha, or 50 % of Pan-Amazon large-scale degradation). Bolivia experienced the highest relative percentage, with 9 % of its remaining intact forest burned, compared to 0.6 % in Brazil (Fig. 1b and Fig. A1 in the Appendix). To a lesser extent, the 2024 increase in forest fires was also observed in countries historically less affected, such as the Guiana Shield countries and Venezuela, where large-scale degradation was, respectively, 6 and 19 times higher than the previous 5-year average (see the Appendix for more details; see also Fig. A2).

Burned forests resulting from fire-driven degradation in the Pan-Amazon region released an estimated 791 ± 86 Mt CO_2 (million tonnes of carbon dioxide equivalent, ± 1 standard deviation) in 2024 – approximately 7 times higher than the annual average of the previous 2 years (117 ± 13 Mt CO_2; see Fig. 2). Brazil was the largest contributor, accounting for 61 % of these emissions, followed by Bolivia with 32 %. In contrast, emissions from deforestation declined from 1044 ± 65 Mt CO_2 in 2022 to 625 ± 38 Mt CO_2 in 2024. Altogether, emissions from deforestation and fire-driven degradation totalled 1416 ± 108 Mt CO_2 in 2024, with burned forests emerging as the dominant source. Comparatively, the latest publication of the Global Carbon Budget (Friedlingstein et al., 2025) also refers to a massive increase in emissions from deforestation and degradation fires in South America in 2024, from 445 Mt CO_2 in 2023 to 1227 Mt CO_2 in 2024, mostly driven by the unusual dry conditions linked to El Niño.

3 Discussion and conclusions

Our analysis presents findings with certain inherent limitations that should be considered during interpretation. The TMF dataset employed may have a tendency to underrepresent the extent of small-scale forest degradation (< 0.09 ha), particularly that resulting from edge effects, selective logging, and low-intensity fire events. These types of non-permanent disturbances can have considerable ecological consequences that may not be fully captured in the data (Bourgoin et al., 2024). Furthermore, differentiating between disturbances caused by degradation processes and those resulting from deforestation posed a challenge, specifically in the context of the 2024 data, as indicated by Vancutsem et al. (2021) due to lack of historical depth in detecting forest recovery following degradation. This overlap in observational characteristics could introduce some level of uncertainty into the precise categorization of forest change. While these limitations suggest a potential for underestimation of the overall impact, our estimates regarding the general scale of the area affected by fires are considered to be reasonably consistent and remain conservative. The broad magnitude of the impacted area is unlikely to be drastically altered by these factors, suggesting that fire remains a significant driver of landscape change within the study area.

In 2024, forest fires became the leading cause of overall forest disturbance across the Pan-Amazon region. These fires not only triggered significant immediate carbon losses but also set in motion long-term ecological degradation.

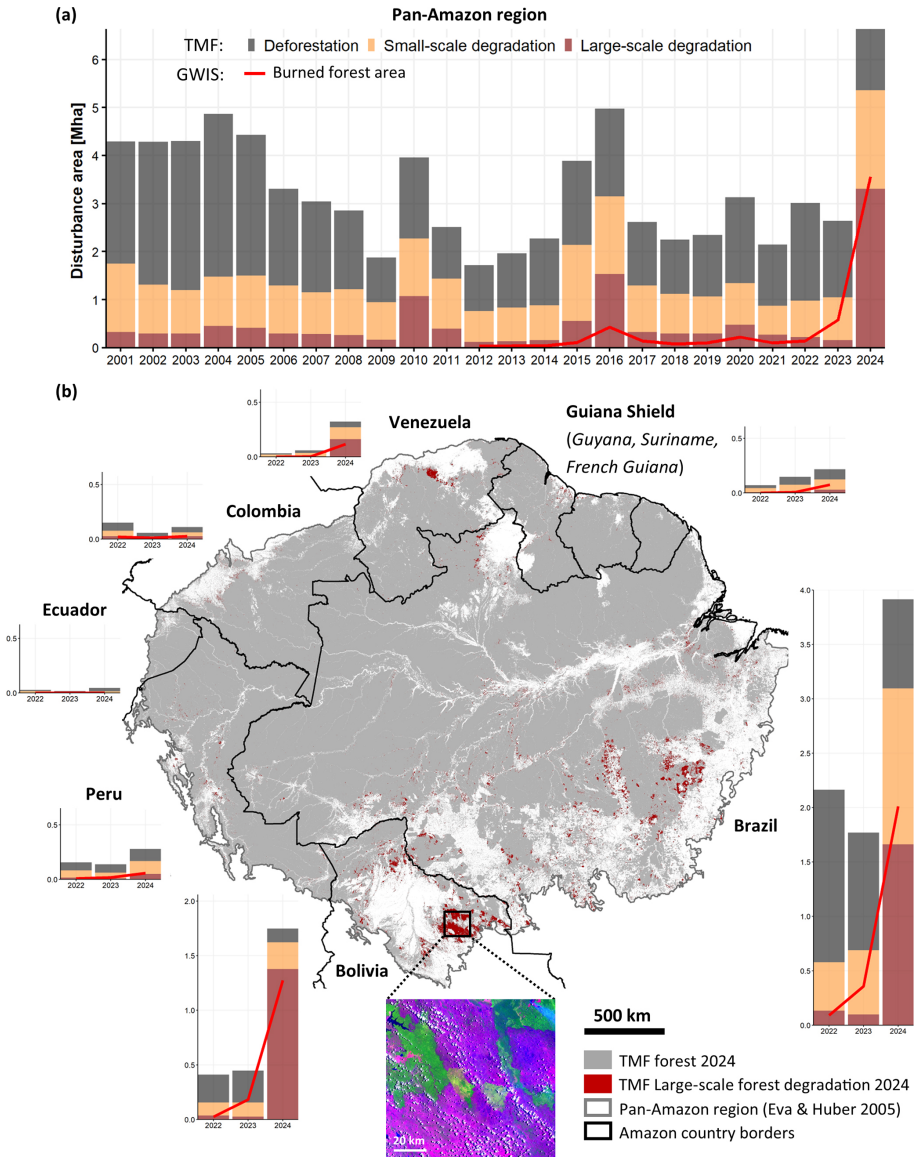

Figure 1. (a) Pan-Amazon Tropical Moist Forest (TMF) Disturbances (2001–2024), including deforestation (dark grey), small-scale degradation (orange), and large-scale degradation (dark red) from the TMF. Burned forest area (red line) represents THE GWIS thermal anomalies overlapping with TMF historical degradation and 2023–2024 TMF disturbances, where THE GWIS detected the fire in the same or previous year. **(b)** Tropical Moist Forest Map: large-scale TMF 2024 forest degradation and recent country forest disturbances (legend and units as in panel **(a)**). The inset shows Landsat-8 imagery (courtesy of the US Geological Survey USGS/NASA), with burn scars in purple and undisturbed forest in green (21 October 2024; RGB: bands 6, 5, 4). The Pan-Amazon region from Eva and Huber (2005) comprises the regions "Amazonia stricto sensu" and "Guiana". Figures A1–A3 provide further details regarding TMF-GWIS data integration and absolute and/or relative forest disturbances at the country level.

This degradation is marked by shifts in forest composition – driven by the limited evolutionary adaptations of Amazonian species to fire – along with persistently high rates of tree mortality. As a result, affected forests may act as a net source of carbon emissions for up to 7 years or more after the fire (Lapola et al., 2023). Climate change, unsustainable land use, and increased forest vulnerability are fuelling a self-reinforcing cycle of escalating fire occurrence and intensity in the Amazon region. This destructive synergy undermines regional forest conservation goals, driving significant forest degradation, particularly during extreme weather events, and potentially leading to permanent shifts in precipitation patterns, including intensified dry seasons along the Amazon's southern, eastern, and northern borders (Hirota et al., 2021).

The 2024 data from Brazil, Bolivia, and Venezuela highlight the Amazon's rapidly decreasing resilience. The uneven

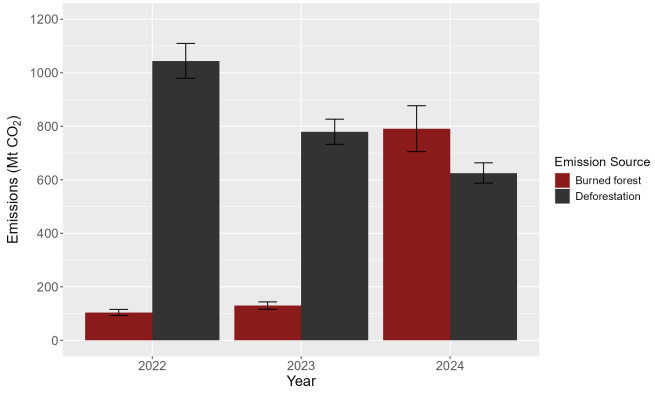

Figure 2. Pan-Amazon emissions from deforestation and fire-driven degradation in 2022–2024. Emissions from small-scale degradation processes (e.g. selective logging) or from disturbances in areas where the GWIS thermal anomalies do not overlap with TMF forest degradation are not included in this analysis. Bars represent the mean values, and vertical error bars indicate the standard deviations, both derived from combining uncertainties using Monte Carlo simulation.

distribution of degradation, coupled with the rising frequency and intensity of forest fires, necessitates robust data-driven mapping approaches and standardized reporting systems to facilitate effective regional coordination and responses (Melo et al., 2023). To address these challenges, it is crucial to prioritize areas of intervention and to develop targeted strategies for reducing deforestation and forest degradation (Lapola et al., 2023). If left unchecked, current trends will push the Amazon forest towards a catastrophic tipping point, irreparably damaging the ecosystem and global climate stability (Flores et al., 2024). Therefore, immediate action is essential to mitigate the underlying drivers of forest fires and to prevent the crossing of this critical threshold.

Appendix A

A1 Tropical Moist Forest dataset

The Tropical Moist Forest (TMF) dataset provides a comprehensive, wall-to-wall mapping of global tropical humid forest cover dynamics from 1990 to 2024 at 30 m spatial resolution using the entire Landsat archive to detect both permanent and temporary forest disturbances. The performance of disturbance detection in Latin America results in 7.1 % omissions, 12.8 % commissions, and 91 % overall accuracy (see Table S3 from Vancutsem et al., 2021).

The TMF system enables analytical separation of forest degradation and deforestation on an annual basis by recording disturbance event timing with a daily temporal resolution, using duration and recurrence as proxies to separate distinct impacts of land use change (i.e. deforestation) from structural and/or functional alterations (i.e. degradation) within forested land (Bourgoin et al., 2024; Beuchle et al., 2021).

Degraded forests are forests that experienced up to three short-duration disturbance events between 1990 and 2023. These short-term events are characterized by a maximum duration of 900 d during which tree foliage cover is absent within a Landsat pixel and is followed by a forest recovery signal (Vancutsem et al., 2021). To qualify as separate events, disturbances must be separated by at least 2 years without any detected disturbances. If more than three of such events occur, the pixel is classified as deforestation, with the year of deforestation being assigned to the start of the first observed disturbance. For 2024, the classification between degradation and deforestation is based on the ratio of valid observations (i.e. pixels free of clouds, haze, and cloud shadows) to observed disturbance events given the insufficient historical depth to determine disturbance permanence. Key drivers of forest degradation include selective logging, wildfires, and natural disturbances such as windthrow and prolonged drought (Vancutsem et al., 2021).

An automated 3×3 pixel moving-window filter was applied to each new forest degradation event, classifying small, isolated patches ($\lesssim 0.8$ ha) associated with log landings, felling gaps, and logging roads (Lima et al., 2020) separately from larger, contiguous patches indicative of fire scars and drought (Morton et al., 2011).

Deforestation is defined as the conversion of an undisturbed or previously degraded forest into another land cover type, indicated by either a single disturbance event lasting more than 900 d or by more than three short-term disturbance events. In both cases, the year of deforestation is assigned to the first year of the relevant disturbance sequence and is mostly driven by agricultural, infrastructure, and mining expansion.

A2 Global Wildfire Information System dataset

The Global Wildfire Information System (GWIS) is a joint initiative of the Group on Earth Observations (GEO) and the Copernicus Work Programs that integrates existing information sources at regional and national levels in order to provide a comprehensive view and evaluation of fire regimes and their impacts at a global level.

The GWIS system is an ecosystem of geographic information system applications used to monitor wildfires globally in near-real time. The core of the system is the Burned Area Near Real Time dataset (GWIS BA NRT), which contains geolocated wildfire events along with associated metadata such as polygons, start and end dates, and various ancillary attributes.

This dataset is derived from thermal anomalies detected by two satellite-based sensors: MODIS (Justice et al., 2002) (on board the TERRA and AQUA satellites) and VIIRS (Schroeder et al., 2014) (on board the SUOMI/NPP and NOAA20 and NOOA21 satellites).

The thermal anomalies covering the entire globe are obtained from the Fire Information for Resource Management System (FIRMS) near-real-time dataset and are stored in a PostGIS database with their geolocation, acquisition date, and other ancillary data unrelated to this topic.

The thermal anomalies are grouped based on their spatial and temporal proximity using the "Spatio-Temporal Density-Based Spatial Clustering of Applications with Noise" algorithm (ST-DBSCAN, Birant and Kut, 2007). The algorithm groups data points into clusters based on their spatio-temporal density, which is calculated using the following parameters: ε (i.e. the maximum spatial distance), εt (i.e. the maximum temporal distance), and minPts (i.e. the minimum number of elements required to start a cluster). Points that do not meet clustering criteria are labelled as noise. For each identified cluster, a circular buffer of 500 m radius is created around each thermal anomaly. These buffers are then merged to create a polygon that approximates the area of the event. The earliest acquisition date among the anomalies defines the start of the fire event, while the latest defines the end.

The dataset used in this study includes detections from the AQUA, TERRA, and SUOMI/NPP satellites, covering the period from 2012 onwards. Based on previous analyses, the clustering parameters applied were $\varepsilon = 1.1$ km, $\varepsilon t = 72$ h, and minPts $= 4$. This means each fire cluster included at least four thermal anomalies, and there were less than 1.1 km and 72 h between neighbouring anomalies. For this analysis, all of the fire events falling in the Pan-Amazon region from Eva and Huber (2005) have been selected from the GWIS dataset for the years 2012 to 2024. This subset includes approximately 553 000 clusters per burnt-area event, with a cumulative burned area of around 250 Mha.

A3 Integration of TMF-GWIS datasets

To isolate burned forest area from GWIS thermal anomaly detections, we performed several spatial and temporal operations using the TMF dataset. A thermal anomaly detected by the GWIS was considered to be burned forest only when the following conditions were met:

- *Spatial overlap with TMF forest degradation (2012–2022)*. The anomaly had to intersect areas classified as forest degradation in the TMF dataset during the 2012–2022 period. This corresponds to short-duration disturbances, specifically one to three events, each lasting less than 900 d (see Appendix A1 for details). GWIS detections within TMF-classified undisturbed forest were excluded from the analysis. This step aims to address potential overestimations in GWIS fire detection due to its clustering and buffering approach (see Appendix A2), as well as potential under-detections in the TMF, particularly of small-scale events (< 0.09 ha) or those without significant canopy change (e.g. understorey fires). Conclusive analysis of these cases requires independent validation, which is beyond this paper's scope; thus, our results remain conservative. GWIS detections occurring on land classified by the TMF as deforested or as other land cover (including areas deforested before 1990) were excluded. These areas are generally associated with deforestation-related fires (e.g. burning debris) or agricultural burning and fall outside the scope of our analysis focused on forest degradation.

- *Temporal consistency with TMF degradation timing.* The fire had to occur in either the same year as the TMF-recorded degradation or the preceding year. This temporal buffer accounts for potential delays in TMF detection due to Landsat's temporal resolution and important cloud cover in some parts of the Amazon region.

- *Overlap with TMF forest disturbance (2023–2024)*. For the 2023–2024 period, anomalies were required to overlap with areas classified as forest disturbance in the TMF. This adjustment acknowledges the current uncertainty in the TMF's ability to distinguish between degradation and deforestation during this recent time frame.

The application of these filters resulted in the exclusion of most GWIS thermal anomaly detections (Fig. A3a), with only 13.7 % of the original dataset remaining. This remaining subset corresponds to approximately 14 Mha of burned forest resulting from fire-driven degradation in Amazonian tropical moist forests. The trend of increasing burned forest area from 2012 to 2024 across different Pan-Amazonian land cover types is shown in Fig. A3b.

A4 Estimation of CO_2 emissions and uncertainty analysis

We estimated carbon dioxide (CO_2) emissions resulting from fire-driven degradation and deforestation in the Amazon basin for the years 2022, 2023, and 2024 using a Monte Carlo simulation framework. Emissions were calculated based on spatially explicit data on change areas and aboveground biomass (AGB) from the 2021 ESA CCI AGB map (Santoro and Cartus, 2024), incorporating uncertainty in all relevant variables, including classification errors in change areas. Burned forest areas from fire-driven degradation were identified through the spatial intersection of TMF forest degradation and GWIS fire detections (as detailed in the "Integration of TMF–GWIS datasets" section), enhancing confidence in the detection of burned forests while yielding a conservative estimate. Areas of deforestation were directly derived from the TMF. For computational efficiency and to minimize the influence of spatial autocorrelation in AGB errors, we aggregated change areas (fire-driven degradation and deforestation), AGB, and its associated standard deviation within spatial units of 0.5° grid cells.

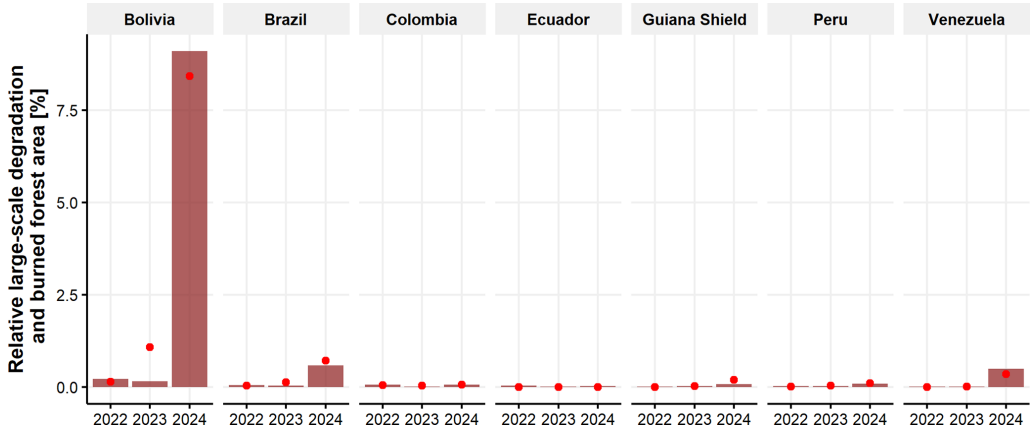

Figure A1. Large-scale degradation relative to intact forest area from the TMF (bars) at the country level within the Pan-Amazon region. Red dots indicate the burned area of tropical moist forest from the TMF-GWIS integration related to the intact forest area from the TMF.

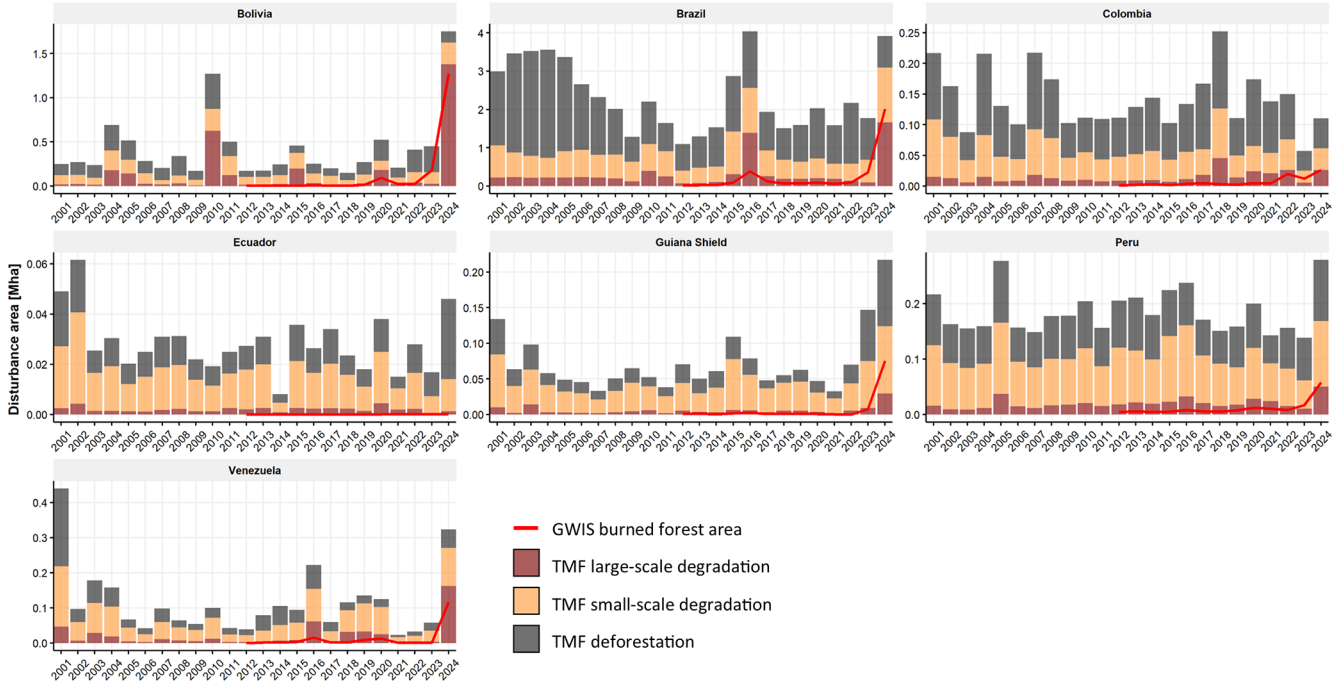

Figure A2. Amazonian forest disturbances from the TMF (2001–2024) and burned forest area from the TMF-GWIS integration (2012–2024) at the country level.

A4.1 Emissions from forest fires

Emissions from fire-affected areas (E_{fire}) were calculated using Eq. (A1), which follows Eq. (2.27) of the 2006 IPCC guidelines (IPCC, 2006) and factors from Tables 2.5 and 2.6 of the 2019 IPCC (IPCC, 2019):

$$E_{\text{fire}} = \sum_{i=1}^{n} A_i^{\text{fire}} \cdot B_i \cdot C_c \cdot G_{\text{ef}} \times 10^{-3}, \quad \text{(A1)}$$

where A_i^{fire} is the adjusted burned forest area (ha) in spatial unit i, B_i is the aboveground biomass (Mg ha^{-1}) in spatial unit i, C_c is the combustion completeness (adimensional), G_{ef} is the emission factor (g CO_2 kg^{-1} dry biomass), n is the number of spatial units, and 10^{-3} just converts g CO_2 into Mg CO_2. The emission factor G_{ef} was sampled from a normal distribution with a mean of 1580 g CO_2 kg^{-1} dry biomass and a standard deviation of 90 g CO_2 kg^{-1} dry biomass based on Andreae and Merlet (2001). Combustion completeness (C_c) was modelled as a normal distribution with a mean of 0.50 and standard deviation of 0.03, consistently with values reported for tropical forest fires (van der Werf et al., 2010).

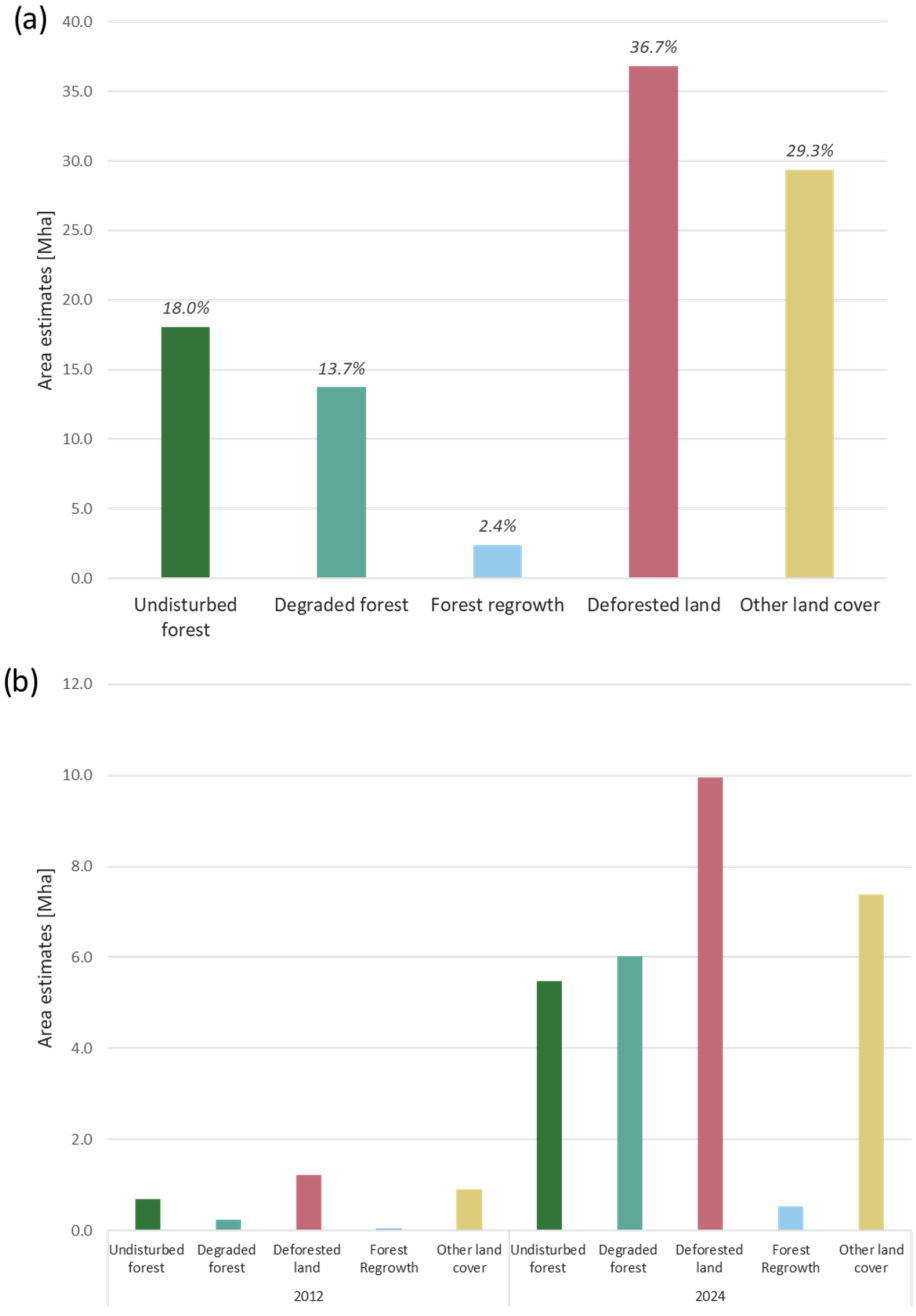

Figure A3. **(a)** Total thermal anomalies (2012–2024) from the GWIS, distributed across the TMF transition classes: undisturbed forest, degraded forest, forest regrowth, deforested land (detected between 1990 and 2024), and other land cover (including areas deforested prior to 1990). **(b)** Annual GWIS thermal anomalies for 2012 and 2024, categorized by TMF annual land cover status, including undisturbed forest, degraded forest, deforested land, forest regrowth, and other land cover types in each respective year.

A4.2 Emissions from deforestation

Emissions from deforestation (E_{defor}) were computed with Eq. (A2):

$$E_{\text{defor}} = \sum_{i=1}^{n} A_i^{\text{defor}} \cdot B_i \cdot C \cdot \left(\frac{44}{12}\right), \quad \text{(A2)}$$

where A_i^{defor} is the adjusted deforested area (ha), C is the carbon fraction of dry biomass (fixed at 0.47), and 44/12 is the molecular weight ratio to convert carbon into CO_2. Unlike fire emissions, no combustion completeness or emission factor is needed for deforestation as it is assumed that all biomass is eventually emitted (IPCC, 2006).

A4.3 Uncertainty in area estimates

To incorporate classification uncertainty in both burned- and deforested-area estimates, we applied probabilistic adjustments to the mapped areas using commission and omission error rates derived from the confusion matrix reported in Vancutsem et al. (2021). These error rates were modelled as Beta distributions to reflect their probabilistic nature, enabling their integration into a Monte Carlo simulation framework. This approach follows best practices for area estimation under classification uncertainty (Olofsson et al., 2014). Specifically, commission error was modelled as $\text{Beta}(\alpha_{\text{cm}} = 8.4, \beta_{\text{cm}} = 91.6)$, and omission error was modelled as $\text{Beta}(\alpha_{\text{om}} = 18.1, \beta_{\text{cm}} = 81.9)$. These distributions were used to adjust the mapped areas of burned and deforested land in each simulation iteration, allowing the uncertainty in classification accuracy to propagate into the final emission estimates. Adjusted areas (A^{adj}) were computed in each iteration of the simulation using Eq. (A3):

$$A^{\text{adj}} = \frac{A \cdot (1 - e_{\text{c}})}{1 - (e_{\text{c}} + e_{\text{o}})}, \tag{A3}$$

where e_{c} and e_{o} are sampled commission and omission errors, respectively.

A4.4 Monte Carlo simulation

We performed 100 000 Monte Carlo iterations per year and source. In each iteration, we simultaneously sampled (i) commission and omission errors (affecting area adjustments) and (ii) AGB values (modelled as normal distributions with the mean and standard deviation derived from the data), combustion completeness, and emission factors for fire emissions only. Negative samples were truncated at zero. The result was a distribution of total CO_2 emissions for each source (fire, deforestation) and year, from which the average and standard deviation were derived.

Code availability. The codes used for running the spatial statistics were written in javascript and R and are available upon request from the corresponding author.

Data availability. All of the data used to download tropical moist forest disturbances and to calculate their trends over the period of 2001–2024 are from the Tropical Moist Forest (TMF) dataset and are accessible via https://forobs.jrc.ec.europa.eu/TMF (last access: 9 July 2025). All of the data used to download the fire detections and calculate their trends are from the Global Wildfire Information System (GWIS) dataset and are accessible via https://gwis.jrc.ec.europa.eu/ (last access: 9 July 2025).

Author contributions. CB: conceptualization, formal analysis, investigation, methodology, writing (original draft). RB: conceptualization, methodology, writing (review and editing). AB: conceptualization, writing (review and editing). JC: conceptualization, investigation, methodology, writing (review and editing). GC: conceptualization, writing (review and editing). DO: conceptualization, methodology, writing (review and editing). JSMA: conceptualization, methodology, writing (review and editing). FS: conceptualization, methodology, writing (review and editing).

Competing interests. The contact author has declared that none of the authors has any competing interests.

Disclaimer. The views expressed are purely those of the writers and may not in any circumstances be regarded as stating an official position of the European Commission.

Publisher's note: Copernicus Publications remains neutral with regard to jurisdictional claims made in the text, published maps, institutional affiliations, or any other geographical representation in this paper. While Copernicus Publications makes every effort to include appropriate place names, the final responsibility lies with the authors.

Acknowledgements. We are grateful for the technical support, feedback, and comments received from Frédéric Achard, Rene Colditz, Andrea Marelli, Silvia Carboni, Dario Simonetti, and Mirco Migliavacca during numerous discussions. The authors utilized AI tools to enhance the readability of the drafts of this paper. Following this, the authors thoroughly reviewed and edited the content as necessary and take full responsibility for the contents of the paper.

Financial support. This study was carried out and financed by the European Union through the European Commission Joint Research Centre and the Directorate-General for International Partnerships (Amazonia+ programme). The Global Wildfire Information System (GWIS) is supported by the European Union Copernicus Work Program.

Review statement. This paper was edited by Sara Vicca and Anja Rammig and reviewed by two anonymous referees.

References

Andela, N., Morton, D. C., Schroeder, W., Chen, Y., Brando, P. M., and Randerson, J. T.: Tracking and classifying Amazon fire events in near real time, Sci. Adv., 8, eabd2713, https://doi.org/10.1126/sciadv.abd2713, 2022.

Andreae, M. O. and Merlet, P.: Emission of trace gases and aerosols from biomass burning, Global Biogeochem. Cy., 15, 955–966, https://doi.org/10.1029/2000GB001382, 2001.

Barlow, J., Berenguer, E., Carmenta, R., and França, F.: Clarifying Amazonia's burning crisis, Glob. Change Biol. 26, 319–321, https://doi.org/10.1111/gcb.14872, 2020.

Beuchle, R., Achard, F., Bourgoin, C., Vancutsem, C., Eva, H., and Follador, M.: Deforestation and forest degradation in the Amazon – Status and trends up to year 2020, EUR 30727 EN, Publications Office of the European Union, Luxembourg, ISBN 978-92-76-38352-9, https://doi.org/10.2760/61682, 2021.

Birant, D. and Kut, A.: ST-DBSCAN: An algorithm for clustering spatial–temporal data, Data Knowl. Eng., 60, 208–221, https://doi.org/10.1016/j.datak.2006.01.013, 2007.

Bourgoin, C., Ceccherini, G., Girardello, M., Vancutsem, C., Avitabile, V., Beck, P. S. A., Beuchle, R., Blanc, L., Duveiller, G., Migliavacca, M., Vieilledent, G., Cescatti, A., and Achard, A.: Human degradation of tropical moist forests is greater than previously estimated, Nature, 631, 570–576, https://doi.org/10.1038/s41586-024-07629-0, 2024.

Cano-Crespo, A., Oliveira, P. J. C., Boit, A., Cardoso, M., and Thonicke, K.: Forest edge burning in the Brazilian Amazon promoted by escaping fires from managed pastures, J. Geophys. Res.-Biogeo., 120, 2095–2107, https://doi.org/10.1002/2015JG002914, 2015.

Condé, T. M., Higuchi, N., and Lima, A. J. N.: Illegal Selective Logging and Forest Fires in the Northern Brazilian Amazon, Forests, 10, 61, https://doi.org/10.3390/f10010061, 2019.

Eva, H. and Huber, O.: A Proposal for defining the geographical boundaries of Amazonia, EUR 21808 EN, Luxembourg, Office for Official Publications of the European Communities, JRC68635, ISBN 92-79-00012-8, https://publications.jrc.ec.europa.eu/repository/handle/JRC68635 (last access: 9 July 2025), 2005.

Flores, B. M., Montoya, E., Sakschewski, B., Nascimento, N., Staal, A., Betts, R. A., Levis, C., Lapola, D. M., Esquível-Muelbert, A., Jakovac, C., Nobre, C. A., Oliveira, R. S., Borma, L. S., Nian, D., Boers, N., Hecht, S. B., ter Steege, H., Arieira, J., Lucas, I. L., Berenguer, E., Marengo, J. A., Gatti, L. V., Mattos, C. R. C., and Hirota, M.: Critical transitions in the Amazon forest system, Nature 626, 555–564, https://doi.org/10.1038/s41586-023-06970-0, 2024.

Friedlingstein, P., O'Sullivan, M., Jones, M. W., Andrew, R. M., Hauck, J., Landschützer, P., Le Quéré, C., Li, H., Luijkx, I. T., Olsen, A., Peters, G. P., Peters, W., Pongratz, J., Schwingshackl, C., Sitch, S., Canadell, J. G., Ciais, P., Jackson, R. B., Alin, S. R., Arneth, A., Arora, V., Bates, N. R., Becker, M., Bellouin, N., Berghoff, C. F., Bittig, H. C., Bopp, L., Cadule, P., Campbell, K., Chamberlain, M. A., Chandra, N., Chevallier, F., Chini, L. P., Colligan, T., Decayeux, J., Djeutchouang, L. M., Dou, X., Duran Rojas, C., Enyo, K., Evans, W., Fay, A. R., Feely, R. A., Ford, D. J., Foster, A., Gasser, T., Gehlen, M., Gkritzalis, T., Grassi, G., Gregor, L., Gruber, N., Gürses, Ö., Harris, I., Hefner, M., Heinke, J., Hurtt, G. C., Iida, Y., Ilyina, T., Jacobson, A. R., Jain, A. K., Jarníková, T., Jersild, A., Jiang, F., Jin, Z., Kato, E., Keeling, R. F., Klein Goldewijk, K., Knauer, J., Korsbakken, J. I., Lan, X., Lauvset, S. K., Lefèvre, N., Liu, Z., Liu, J., Ma, L., Maksyutov, S., Marland, G., Mayot, N., McGuire, P. C., Metzl, N., Monacci, N. M., Morgan, E. J., Nakaoka, S.-I., Neill, C., Niwa, Y., Nützel, T., Olivier, L., Ono, T., Palmer, P. I., Pierrot, D., Qin, Z., Resplandy, L., Roobaert, A., Rosan, T. M., Rödenbeck, C., Schwinger, J., Smallman, T. L., Smith, S. M., Sospedra-Alfonso, R., Steinhoff, T., Sun, Q., Sutton, A. J., Séférian, R., Takao, S., Tatebe, H., Tian, H., Tilbrook, B., Torres, O., Tourigny, E., Tsujino, H., Tubiello, F., van der Werf, G., Wanninkhof, R., Wang, X., Yang, D., Yang, X., Yu, Z., Yuan, W., Yue, X., Zaehle, S., Zeng, N., and Zeng, J.: Global Carbon Budget 2024, Earth Syst. Sci. Data, 17, 965–1039, https://doi.org/10.5194/essd-17-965-2025, 2025.

Hirota, M., Flores, B. M., Betts, R., Borma, L. S., Esquível-Muelbert, A., Jakovac, C., Lapola, D. M., Montoya, E., Oliveira R. S., and Sakschewski, B.: Chapter 24: Resilience of the Amazon Forest to Global Changes: Assessing the Risk of Tipping Points, https://doi.org/10.55161/QPYS9758, 2021.

IPCC: IPCC Guidelines for National Greenhouse Gas Inventories Vol. 4, edited by: Eggleston, H. S., Buendia, L., Miwa, K., Ngara, T., and Tanabe, K., IGES, 2006, 11, ISBN 4-88788-032-4, 2006.

IPCC: Refinement to the 2006 IPCC Guidelines for National Greenhouse Gas Inventories, Vol. 4, edited by: Buendia, E., Tanabe, K., Kranjc, A., Baasansuren, J., Fukuda, M., Ngarize, S., Osako, A., Pyrozhenko, Y., Shermanau, P., and Federici, S., ISBN 978-4-88788-232-4, 2019.

Justice, C. O., Giglio, L., Korontzi, S., Owens, J., Morisette, J. T., Roy, D., Descloitres, J., Alleaume, S., Petitcolin, F., and Kaufman, Y.: The MODIS fire products, Remote Sens. Environ., 83, 244–262, https://doi.org/10.1016/S0034-4257(02)00076-7, 2002.

Kornhuber, K., Bartusek, S., Seager, R., Schellnhuber, H. J., and Ting, M.: Global emergence of regional heatwave hotspots outpaces climate model simulations, P. Natl. Acad. Sci. USA, 121, e2411258121, https://doi.org/10.1073/pnas.2411258121, 2024.

Lapola, D. M., Pinho, P., Barlow, J., Aragão, L. E. O. C., Berenguer, E., Carmenta, R., Liddy, H. M., Seixas, H., Silva, C. V. J., Silva-Junior, C. H. L., Alencar, A. A. C., Anderson, L. O., Armenteras, D., Brovkin, V., Calders, K., Chambers, J., Chini, L., Costa, M. H., Faria, B. L., Fearnside, P. M., Ferreira, J., Gatti, L., Gutierrez-Velez, V. H., Han, Z., Hibbard, K., Koven, C., Lawrence, P., Pongratz, J., Portela, B. T. T., Rounsevell, M., Ruane, A. C., Schaldach, R., da Silva, S. S., von Randow, C., and Walker, W. S.: The drivers and impacts of Amazon forest degradation, Science, 379, eabp8622, https://doi.org/10.1126/science.abp8622, 2023.

Lima, T. A., Beuchle, R., Griess, V. C., Verhegghen, A., and Vogt, P.: Spatial patterns of logging-related disturbance events: a multi-scale analysis on forest management units located in the Brazilian Amazon, Landscape Ecol., 35, 2083–2100, https://doi.org/10.1007/s10980-020-01080-y, 2020.

Matricardi, E. A. T., Skole, D. L., Pedlowski, M. A., and Chomentowski, W.: Assessment of forest disturbances by selective logging and forest fires in the Brazilian Amazon using Landsat data, Int. J. Remote Sens., 34, 1057–1086, https://doi.org/10.1080/01431161.2012.717182, 2012.

Marengo, J., Cunha, A., Espinoza, J., Fu, R., Schöngart, J., Jimenez, J., Costa, M., Ribeiro, J., Wongchuig, S., and Zhao, S.: The Drought of Amazonia in 2023–2024, Am. J. Clim. Change, 13, 567–597, https://doi.org/10.4236/ajcc.2024.133026, 2024.

Melo, J., Baker, T., Nemitz, D., Quegan, S., and Ziv, G.: Satellite-based global maps are rarely used in forest reference levels submitted to the UNFCCC, Environ. Res. Lett., 18, 034021, https://doi.org/10.1088/1748-9326/acba31, 2023.

Morton, D. C, DeFries, R. S., Nagol, J., Souza, C. M., Kasischke, E. S., Hurtt, G. C., and Dubayah, R.: Mapping canopy damage from understory fires in Amazon forests using annual time series of Landsat and MODIS data, Remote Sens. Environ., 115, 1706–1720, https://doi.org/10.1016/j.rse.2011.03.002, 2011.

Olofsson, P., Foody, G. M., Herold, M., Stehman, S. V., Woodcock, C. E., and Wulder, M. A.: Good practices for estimating area and assessing accuracy of land change, Remote Sens. Environ., 148, 42–57, https://doi.org/10.1016/j.rse.2014.02.015, 2014.

Rorato, A. C, Escada, M. I. S., Camara, G., Picoli, M. C. A., and Verstegen, J. A.: Environmental vulnerability assessment of Brazilian Amazon Indigenous Lands, Environ. Sci. Pol., 129, 19–36, https://doi.org/10.1016/j.envsci.2021.12.005, 2022.

San-Miguel, J., Durrant, T., Suarez-Moreno, M., Oom, D., Branco, A., Libertà, G., De Rigo, D., Ferrari, D., Roglia, E., Scionti, N., Maianti, P., Boca, R., Broglia, M., Callisaya, F., Cerezo, R., Monasterios, G., Santos, L. Q., Claure, A., Nobrega De Oliveira, L., Senra De Oliveira, M., Terra, G., Morita, J. P., Marcon Silva, M., Setzer, A., Morelli, F., Libonati, R., Bernini, H., Lobos Stephani, P. A., Saavedra Salinas, J. A., Brull Badia, J., Garzon Cadena, N., Arenas Aguirre, M. A., Avila, K., Solano, L., Lancheros, S., Puerto Prieto, J. C., Jader Ocampo, J., Vargas Hernandez, M., Gonzalo Murcia, U., Arias, J., Rodriguez Leon, A., Moreno, L. M., Diana, S., Pazmiño, J., Cobos, S., Segura, D., Herrera, X., Sarango, C., Quispillo, M., Arrega Diaz, C., Cruz, E., Salgado, T., Toffoletti, M., Pereira Gavilan, R., Alarco Basaldua, G. E., Zarella Pequeño Saco, T., Epiquien Rivera, J. L., Canales Campos, W. L., Liza Contreras, R. A., Ricalde Bellido, C., Zubieta Barragan, R., Saavedra Estrada, R. M., Sono Alba, S., Ramirez Arroyo, R., Diaz Escobal, E., Albornoz Yañez, M., Casaretto Gamonal, M., Rosas, G., Quispe, N., Gonzales Figueroa, J., Cueva Melgar, E. L., Salinas, C., Ocampo, I., Ruffino, M., Riaño, R., Rico, S., and Escudero, P.: Forest Fire Information and Management Systems in Latin America and the Caribbean, European Union Publications Office, Luxembourg, JRC134498, https://doi.org/10.2760/454551, 2023.

Santoro, M. and Cartus, O.: ESA Biomass Climate Change Initiative (Biomass_cci): Global datasets of forest above-ground biomass for the years 2010, 2015, 2016, 2017, 2018, 2019, 2020 and 2021, v5.01, NERC EDS Centre for Environmental Data Analysis [data set], https://doi.org/10.5285/bf535053562141c6bb7ad831f5998d77, 2024.

Schroeder, W., Oliva, P., Giglio, L., and Csiszar, I. A.: The New VIIRS 375m active fire detection data product: Algorithm description and initial assessment, Remote Sens. Environ., 143, 85–96, https://doi.org/10.1016/j.rse.2013.12.008, 2014.

Vancutsem, C., Achard, F., Pekel, J. F., Vieilledent, G., Carboni, S., Simonetti, D., Gallego, J., Aragão, L. E. O. C., and Nasi, R.: Long-Term (1990–2019) Monitoring of Forest Cover Changes in the Humid Tropics, Sci. Adv., 7, eabe1603, https://doi.org/10.1126/sciadv.abe1603, 2021.

van der Werf, G. R., Randerson, J. T., Giglio, L., Collatz, G. J., Mu, M., Kasibhatla, P. S., Morton, D. C., DeFries, R. S., Jin, Y., and van Leeuwen, T. T.: Global fire emissions and the contribution of deforestation, savanna, forest, agricultural, and peat fires (1997–2009), Atmos. Chem. Phys., 10, 11707–11735, https://doi.org/10.5194/acp-10-11707-2010, 2010.